Proceedings of the ICBBG2025
2025 International conference on Bio-mediated and Bio-inspired Geotechnics
18-20 May, 2025 | Tempe, Arizona, USA
https://doi.org/10.53243/ICBBG2025-99

Plant Root-inspired Penetration Experiments in Layered Sand Profiles

Riya Anilkumar[1] and Alejandro Martinez, Ph.D.[2]

[1]Department of Civil and Environmental Engineering, University of California Davis, California 95616; E-mail: ranilkumar@ucdavis.edu
[2]Department of Civil and Environmental Engineering, University of California Davis, California 95616; E-mail: amart@ucdavis.edu

ABSTRACT

Soil characterization is a vital step preceding the development of any site. During site investigation (SI) activities, penetration through stiff or deep layers poses challenges due to the required large vertical reaction forces. To provide these, rigs for SI are typically large and heavy, creating challenges in accessing sites or with soft surficial soils, increasing mobilization costs and carbon footprint. This paper investigates a plant root-inspired strategy called circumnutation-inspired (CI) penetration which reduces the vertical penetration resistance. The CI probes have a bent tip and are rotated and vertically advanced at constant rates while recording the mobilized forces (F_z) and torques (T_z). CI penetration in layered deposits were investigated by performing a set of tests at varying relative velocities, defined by the ratio of tangential to vertical velocity of the tip of the CI probe ($\omega R/v$). The F_z and T_z mobilized in the layered deposit are compared with those mobilized in respective uniform sand deposits that make up the layered deposit. Cone Penetration Test (CPT) soundings were performed in each of these deposits as well. In all cases, CI penetration resulted in an exponential decrease in F_z with increasing $\omega R/v$, while the T_z increases with initial increases in $\omega R/v$ before reaching a stable value. Both CPT and non-rotational CI penetration mobilize similar F_z in the layered and uniform sand deposits. The total work done during CI penetration at low $\omega R/v$ in layered and uniform deposits has similar magnitudes as conventional testing (98-118% of CPT), while mobilizing significantly lower F_z (46-65% of CPT). Thus, CI penetration can facilitate the use of more compact and lightweight rigs to conduct SI tasks, such as classifying soils or installing sensors.

INTRODUCTION

Soil penetration is crucial for soil characterization in geotechnical investigations and other fields, including agriculture, environmental monitoring, ecology, and climate change (Guireli Netto et al., 2020; Moraes et al., 2014). Standard geotechnical soil characterization methods, such as Cone Penetration Tests (CPT) and Dilatometer Tests (DMT), often encounter difficulties in generating sufficient vertical reaction forces to penetrate deep or dense soil layers, resulting in early termination of tests (Jamiolkowski, 2012). To address this issue, larger and heavier rigs are typically employed to provide the necessary vertical reaction forces. However, these rigs pose additional challenges related to the carbon footprint of mobilization, transportation costs, and reaching sites with limited accessibility or soft surficial layers (Purdy et al., 2022). Strategies to mobilize lower vertical resistances would facilitate the use of smaller, light-weight rigs to overcome these challenges.

Organisms that interact with soil have developed efficient ways to penetrate soils over millions of years of evolution. Recent developments have taken inspiration from these natural adaptations to develop more efficient soil penetration strategies for soil characterization (Martinez et al., 2022; Martinez et al. 2024). Chen et al. (2021) and Isava & Winter (2016) investigate radially expanding a portion of the probe (anchor) to provide vertical reaction forces during penetration, facilitating the development of self-burrowing probes. Chen et al. (2024) performed numerical simulations to investigations oscillatory motions of the probe tip to aid penetration. Bengough et al. (1997), Tang & Tao (2022), and Yang et al. (2024) investigated rotational CPT probes while Anilkumar et al. (2024), Chen & Martinez (2024), and Del Dottore et al. (2017) performed tests with CI-inspired rotating probes to reduce the soil vertical resistances and work done during penetration. Apart from CI motion, plants have been shown to reduce the penetration resistance by releasing exudates or growing radially (Oleghe et al. 2017; Bengough et al. 1994).

This study draws inspiration from a strategy observed in plant roots called circumnutation, an autonomous movement where the root tip, which is slightly bent, rotates as it penetrates the soil (Figure 1a). A CI probe was fabricated as a cylindrical probe with a conical tip that has a bent end characterized by the bend angle (α) and bent length (L_1), as shown in Figure 1b. The CI probe is rotated while it is vertically advanced into the soil. The trajectory of the helical path traced by the tip of the probe (Figure 1c) is governed by the relative velocity, defined as the ratio of the tangential velocity (ωR) to vertical velocity (v) of the tip of the probe.

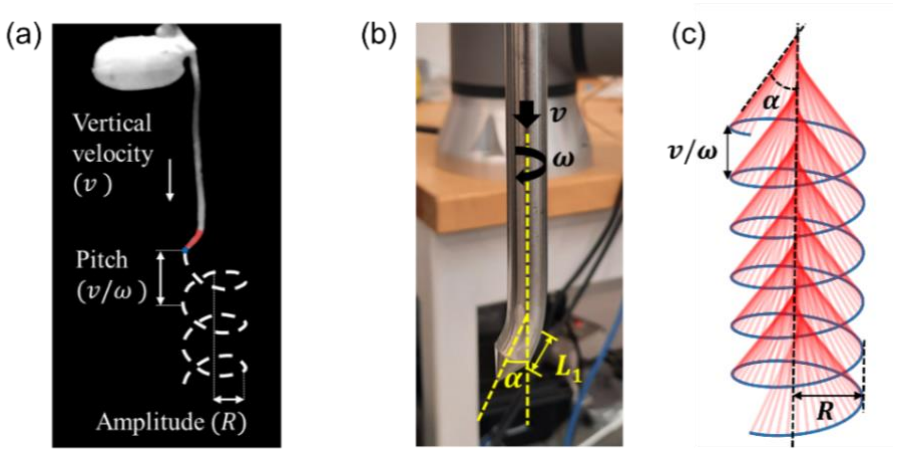

Figure 1: (a) Circumnutation motion exhibit by a rice plant root (modified from Taylor et al. 2021). (b) Circumnutation-inspired probe used for experimental investigations. (c) Trajectory of the central line of the bent end of the circumnutation-inspired probe (in red) and the tip of the probe (in blue).

Previous studies that investigated CI strategies for soil penetration show that increased angular velocity reduces the vertical resistance and within a certain range slightly decreases the work done. Numerical simulations by Chen & Martinez (2024) demonstrated that the ωR/v of the probe controls the resistance and work involved in CI penetration. Experimental investigations performed byDel Dottore et al. (2017), Anilkumar & Martinez (2024a), and Anilkumar & Martinez (2024b) highlighted consistent variations of mobilized forces and work done in uniform soils, including deposits with varying sand density and soil type. This study explores CI penetration in shallow layered sand deposits considering the variation of vertical forces and torques with

increasing relative velocity. The results are then compared with corresponding tests in uniform sand deposits.

MATERIALS AND METHODS

A CI probe with a fixed geometry is used to perform experiments in layered sand deposits. The CI probe used in this study has a diameter (D) of 12.7 mm, an L_1 equal to 1D (i.e., 12.7 mm) and an α = 10°. These values were chosen based on the results of Chen and Martinez (2023) and Anilkumar and Martinez (2024b) who tested a broader range of L_1 and α values. The probe is fabricated from aluminum tubing and its conical tip has an apex angle of 60°. All tests were performed with a spacing of 10 to 12D between adjacent testing locations or between testing location and the container wall to prevent boundary effects. Relative velocities ($\omega R/v$) between 0 and 2 π were used as they are representative for the range observed in different plant species (Chen and Martinez 2023). The probe is moved downwards at a velocity v by a UR16e robotic arm (Universal Robots) and rotated at an angular velocity ω by a stepper motor (Teknic ClearPath NEMA 23) and a gearbox (Carson Manufacturing S-Series Planetary) while the F_z and T_z are measured with a NET six-axis load cell (ATI Industrial Automation) (Figure 2a). Tests with different $\omega R/v$ are obtained by maintaining v constant and changing ω. Tests with a CPT probe with the same diameter and apex angle as the CI probe were performed at the same vertical velocity as the CI tests for comparison.

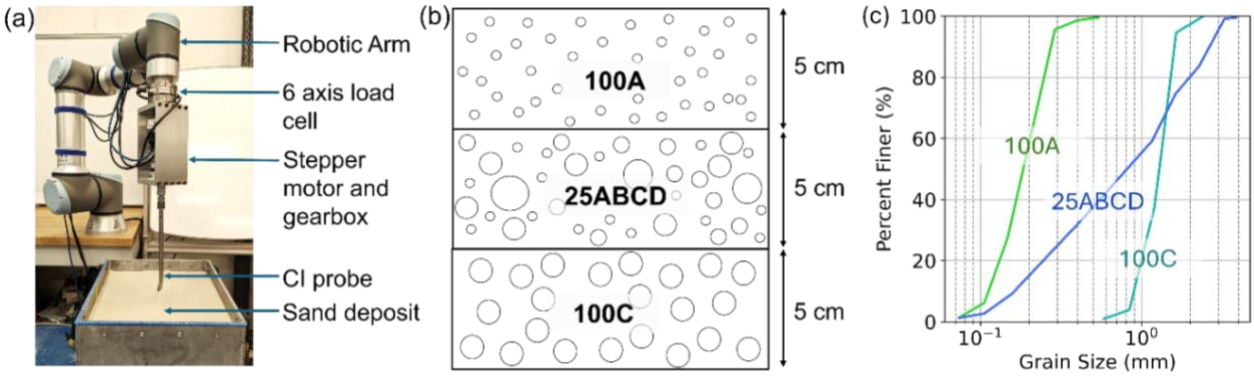

Figure 2: (a) Test setup for the experimental investigations. (b) Schematic of the layered soil profile used for the first set of tests. (c) Particle size gradation of the three sands used in the experimental investigation.

The total depth of penetration in tests was 15 cm. The first set of tests were conducted on sand deposits with layers of equal height, comprising of sand with varying grain size distributions. The layered deposit consisted of uniform fine-grained sand (100A) as the top layer, well-graded sand as the middle layer (25ABCD), and uniform coarse-grained sand (100C) as the bottom-most layer, as shown in Figure 2b. Figure 2c shows the grain size distributions of these sands, and Ahmed et al. (2023) presents a detailed characterization of the triaxial shearing behavior. Table 1 shows the properties of the sands. Each of the layers were prepared at uniform target relative densities of 40% using air pluviation from a fixed drop height. Three additional sets of tests were performed in uniform sand deposits of 100A, 25ABCD and 100C at target D_R of 40% for comparison with the resistances mobilized in the layered sand deposit. Repeated CI tests in the uniform deposits reveal variations in vertical force smaller than 15% and of torque smaller than

0.01 Nm; therefore, the trends reported are not considered to be influenced by experimental variability.

Table 1: Properties of sands used in the study

Properties	100A	25ABCD	100C
10th percentile particle size, D_{10} (mm)	0.12	0.16	0.91
Median particle diameter, D_{50} (mm)	0.18	0.8	1.31
Coefficient of curvature, C_C	1.02	0.67	1.02
Coefficient of uniformity, C_U	1.68	7.44	1.54
Critical state friction angle, ϕ'_{cs}	32.1	33.7	32.1

Ci Penetration In Layered Sand Deposit.

The first set of tests on the layered sand deposit was performed to investigate the effect of $\omega R/v$ on the mobilized F_z and T_z. The v, ω, and $\omega R/v$ used in all tests are presented in Table 2. These results are compared to those obtained from CPT soundings in the same deposit. The F_z and T_z mobilized during CPT and CI penetration in the layered deposit increase with depth. The magnitude of mobilized F_z decreases significantly as $\omega R/v$ is increased, while the F_z generated during CPT and non-rotation CI penetration have similar magnitudes (Figure 3a). The T_z increases from negligible values for the non-rotating probes (i.e., 0.0 π CI penetration and CPT penetration) to higher magnitudes with initial increase in $\omega R/v$, but further increases result in similar magnitudes (Figure 3b). The above-mentioned trends in F_z and T_z with $\omega R/v$ are consistent at all depths. There is no strong trend in the change in F_z and T_z as the probe penetrates the different sand layers as their sensing and development distances are likely larger than the layer thickness of 5 cm, which are approximately equal to 4D. Using the Boulanger & DeJong (2018) sensing distance charts for the top and middle layers, the greatest distance between the probe tip and the top of an underlying layer for which the F_z is affected (i.e., sensing distance) is estimated to be around 6D in the 100A layer and 8D in the 25ABCD layer. Using the Boulanger & DeJong (2018) development distance charts for the middle and bottom layers, the greatest distance between the bottom of the overlying layer and the probe tip for which the F_z is affected (i.e., development distance) is around 3D in the 25ABCD layer and around 5D in the 100C layer. Thus, in the layered sand deposit, the F_z in each layer is likely influenced by the adjacent layers.

Table 2: Test variations for each sand deposit.

Test No	Probe Type	v (mm/s)	ω (RPM)	$\omega R/v(\pi)$
1	CPT	0.5	0	0
2	CI	0.5	0	0
3	CI	0.5	0.91	0.25
4	CI	0.5	1.82	0.5
5	CI	0.5	7.29	2

The cumulative vertical (W_V), rotational (W_R) and total work (W_T) done to penetrate a fixed depth of sand is computed as given by equations 1-3.

$$W_V = \sum_{d_i}^{d_f} F_Z v \Delta t \quad (1)$$

$$W_R = \sum_{d_i}^{d_f} T_Z \omega \Delta t \quad (2)$$

$$W_T = W_V + W_R \quad (3)$$

where d_i is the initial depth, d_f is the final depth, and Δt is the time difference between subsequent data points. Since the W_V and W_R are computed as the incremental sum of the product of F_z and T_z with the corresponding vertical and rotational displacements through the depth of penetration, both increase monotonically with depth (Figure 3c and 3d). The transition depths between layers are also not prominent in the variations of work components. The W_V and W_R done to penetrate a certain depth have contrasting trends with increasing $\omega R/v$, where W_V decreases and W_R increases. These trends are consistent with depth as well.

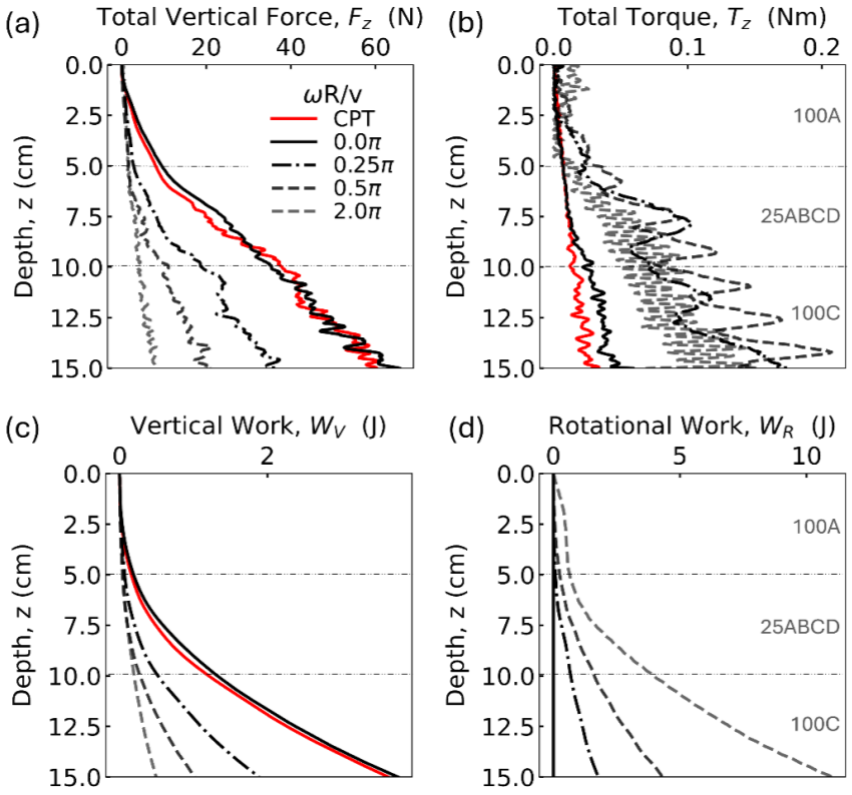

Figure 3: Variation of (a) vertical force, F_z (b) torque, T_z (c) vertical work, W_V, and (d) rotational work W_R with $\omega R/v$ in the layered sand deposit (100A top, 25ABCD middle, 100C bottom).

Comparison To Penetration In Uniform Sand Deposits.

The F_z and T_z mobilized in the layered deposits are compared with tests performed in uniform sand deposits that make up each of the sand layers. CPT and non-rotational CI penetration tests in the uniform deposits show that F_z increases with depth in a similar fashion as the tests on the layered deposit (Figure 4a and 4b). In general, the F_z in the layered deposit is between that mobilized by the strongest (25ABCD) and weakest (100A) deposit. The F_z magnitudes mobilized during CPT and non-rotational CI penetration are similar to one another in both the layered and uniform sand deposits. In comparison to the uniform 100A deposit, the rate of increase in F_z with depth in the layered deposit increases slightly at the first transition zone, between the 100A and 25ABCD sands, while the difference in slope at the second transition

zone, between 25ABCD and 100C sand, is not as prominent. The F_z and T_z mobilized during CI penetration at varying $\omega R/v$ depict similar trends in the layered and uniform deposits (Figures 5a to 5f). The F_z and T_z mobilized in the top layer (100A) have similar magnitudes as those obtained in the uniform 100A deposit while those mobilized in the next two layers are similar or higher in magnitude than those mobilized in uniform 100C but lower than those mobilized in uniform 25ABCD deposits.

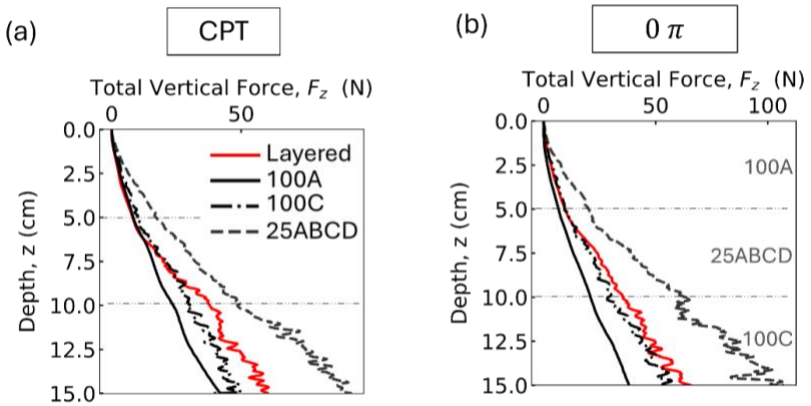

Figure 4: Variation of vertical force, F_z during (a) CPT tests, (b) non-rotational CI penetration in layered sand deposit (100A top, 25ABCD middle, 100C bottom) and uniform deposits of 100A, 25ABCD and 100C sand.

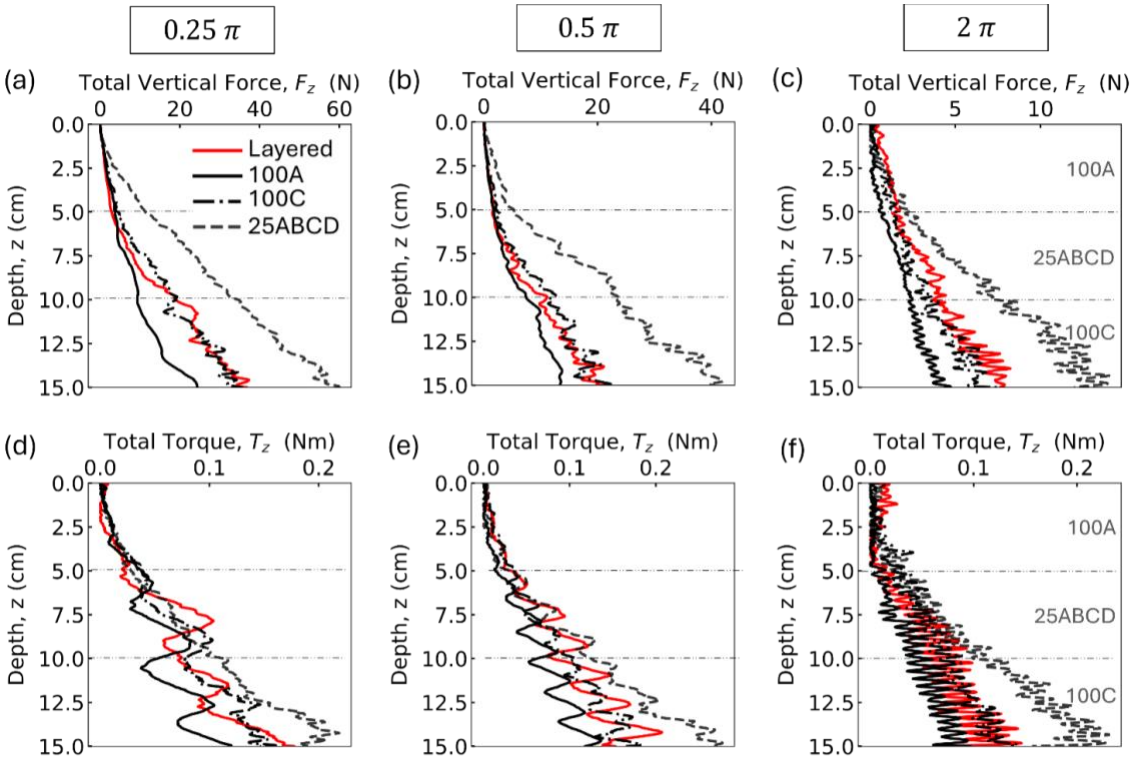

Figure 5: Variation of (a) vertical force, F_z (b) torque, T_z (c) vertical work, W_V, and (d) rotational work W_R with $\omega R/v$ in the layered sand deposit (100A top, 25ABCD middle, 100C bottom) and uniform deposits of 100A, 25ABCD and 100C sand.

DISCUSSION

Given the consistency of F_z and T_z trends with depth, the average values across the different layers are considered to examine their variation with $\omega R/v$. The first layer is excluded in this analysis as the initial few centimetres of penetration may have inconsistencies due to the partial penetration of the probe and boundary effects due to the free-soil surface. The resistances mobilized at any particular depth in the layered deposit vary from the those mobilized in the corresponding uniform deposits as the resistances are mobilized by larger volumes of soil and are thus influenced by the adjacent sand layers (Figure 6a and 6b). The average F_z mobilized in the middle layer of 25ABCD sand of the layered deposit (depth ranging from 5-10 cm) exponentially decreases as the $\omega R/v$ is increased (Figure 6a), in a similar fashion as those mobilized at similar depths in the uniform deposits. The average T_z during penetration of this layer increases considerably with an initial increase in $\omega R/v$, while further increases yield slight reductions, similar to the trends obtained in the uniform deposits (Figure 6b). The magnitude of average F_z and T_z mobilized at this depth in the layered profile is in between those mobilized in uniform 100A and 25ABCD sand deposits. The average F_z and T_z mobilized during CPT penetration in the same depth range have similar magnitudes as those mobilized during non-rotational CI penetration. The average F_z and T_z mobilized during penetration in the bottom layer of the layered deposit follow similar trends as the middle layer, with similar or slightly higher magnitudes than the 100C sand uniform deposit.

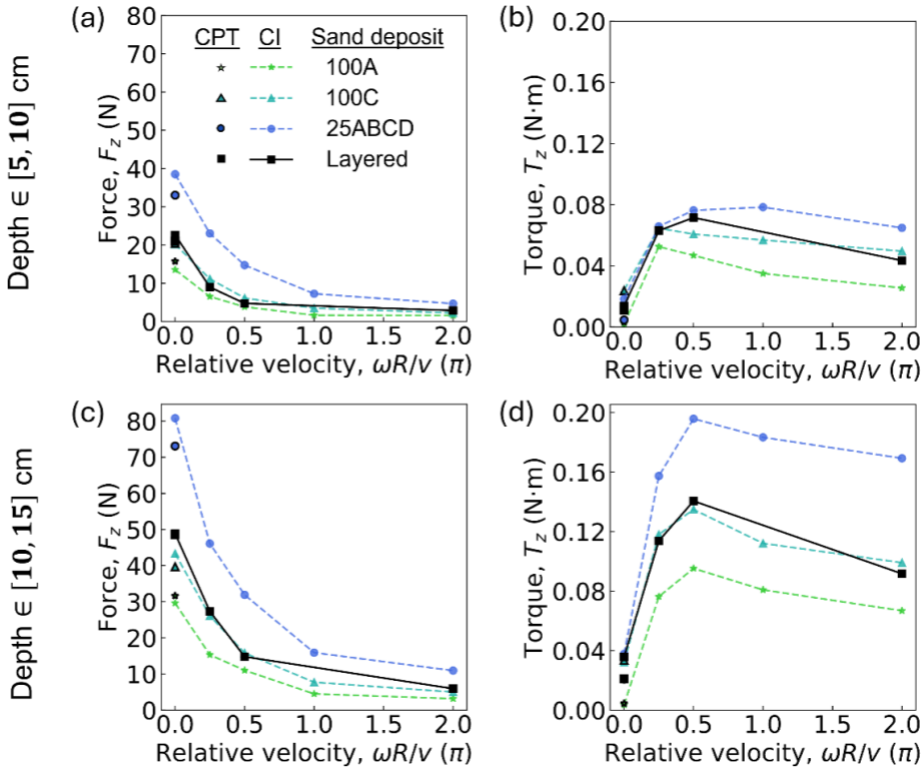

Figure 6: Variation of average (a) vertical force, F_z (b) torque, T_z with $\omega R/v$ during penetration between 5-10 cm. Variation of average (a) vertical force, F_z (b) torque, T_z with $\omega R/v$ during penetration between 10-15 cm.

The cumulative total work done during penetration through the entire soil deposit is computed along with the vertical and rotational components of work using Equations 1 to 3. For all soil deposits the W_V and W_R show opposite trends with $\omega R/v$, where W_V exponentially decays and W_R monotonically increases (Figure 7a and 7b), leading to small initial W_T variations followed by a steady increase at larger $\omega R/v$ (Figure 7c). Since all the tests were performed at a constant vertical velocity and depth of penetration, W_V follows the same trends as the average F_z. While the T_z magnitudes vary slightly for different non-zero $\omega R/v$, increasing ω due to the increase in $\omega R/v$ results in greater rotational displacements (i.e., $\omega \Delta t$), which produce a monotonic increase in W_R. The variation of W_T with $\omega R/v$ is governed by rate of change of W_V and W_R, where the influence of W_V decreases as $\omega R/v$ is increased while the influence of W_R steadily increases. The initial stagnation of the magnitude of W_T at small $\omega R/v$ is due to the similar rate of change in W_V and W_R with increasing $\omega R/v$. The W_V, W_R and W_T done during penetration in the layered deposit lie between the respective bounds of work components from in the uniform deposits. The W_V, W_R and W_T done during CPT penetration is similar to those done during non-rotational CI penetration (i.e., at $\omega R/v$ of 0 π).

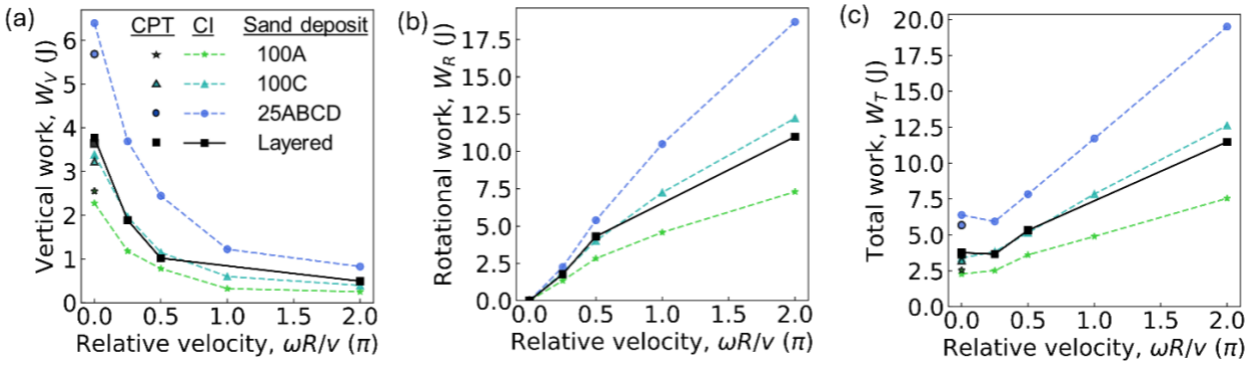

Figure 7: Variation of (a) vertical force, F_z (b) torque, T_z (c) vertical work, W_V, and (d) rotational work W_R with $\omega R/v$ in the layered sand deposit.

Irrespective of the soil profile, the total work done during CI penetration has similar magnitudes with initial increase in $\boldsymbol{\omega R/v}$ while $\boldsymbol{F_z}$ exponentially decays with an increase in $\boldsymbol{\omega R/v}$. This indicates that CI penetration requires a similar amount of work done compared to a CPT sounding while significantly decreasing the mobilized vertical resistance. For example, at an $\boldsymbol{\omega R/v}$ of 0.25 $\boldsymbol{\pi}$, the total work done during CI penetration is less than 20% greater than that done during CPT, while mobilizing about 50% of the vertical force mobilized by the CPT sounding (46% for 100A, 65% for 25ABCD, 61% for 100C and 52% for layered deposit). The variations of $\boldsymbol{F_z}$, $\boldsymbol{T_z}$ and $\boldsymbol{W_T}$ with $\boldsymbol{\omega R/v}$ are consitent with other studies on CI penetration (Anilkumar and Martinez, 2024a, Anilkumar and Martinez, 2024b, Del Dottore et al., 2017). This comparison provides encouraging results for enabling the use of smaller, lightweight rigs while limiting the total work done for SI activities by means of CI penetration.

CONCLUSION

This study explores the circumnutation root-inspired strategy for penetration in shallow, layered sand deposits. The resistances mobilized in CI tests are compared to those from traditional CPT penetration in the same deposits. Results from CI and CPT soundings in uniform sand deposits

allow examining the effect of the layering in the penetration results. The F_z and T_z mobilized in the layered and uniform sand deposits during CI and CPT penetration were analyzed and the associated mechanical work components were computed.

The penetration resistances from CI tests in uniform and layered deposits have similar trends. CI penetration deposits show an exponential decay in F_z as $\omega R/v$ is increased, while T_z increases significantly with initial increase and has minor increases with further increase in $\omega R/v$. The average F_z and T_z mobilized in the different layers of the layered deposit are within the range mobilized in the uniform deposits. The forces and torques in CI tests increase with depth in a similar fashion as in CPT soundings. The F_z and T_z during both CPT and CI penetration in the layered model do not significantly change between layers, likely due to the relatively small layer thickness.

The cumulative work components during penetration in layered deposits show similar trends as those in the uniform deposits. The W_V exponentially decays and the W_R monotonically increases as $\omega R/v$ is increased. The W_T has minor changes in magnitude with initial increase in $\omega R/v$, but increases at higher rates with further increase in $\omega R/v$. Due to this initial stagnation in W_T, CI penetration at small $\omega R/v$ can significantly lower the penetration resistance (i.e., 46-65% of CPT) while requiring similar amount of work done (i.e., 98-118% of CPT) as conventional testing. This can facilitate the use of smaller, lightweight rigs for soil penetration. To enable integration into SI applications, further research should evaluate the effects of depth, confining stresses, and soil types on the penetration resistance and work done during CI penetration.

ACKNOWLEDGMENT

The authors express their gratitude to Fabian Zamora, Junhan Li, Breiner Rodas, Antonia Vezzoli and Xiaotong Yang, for their help in the preparation of the sand deposits. Additionally, the authors extend their appreciation to the faculty and staff at the UC Davis Centre of Geotechnical Modelling (CGM) for their invaluable support, which played a crucial role in making the experimental setup feasible. This material is based upon work supported in part by the Engineering Research Center Program of the National Science Foundation under NSF Cooperative Agreement No. EEC–1449501. The authors were supported by the National Science Foundation (NSF) under Award No. 1942369.

REFERENCES

Ahmed, S. S., Martinez, A., & DeJong, J. T. (2023). Effect of Gradation on the Strength and Stress-Dilation Behavior of Coarse-Grained Soils in Drained and Undrained Triaxial Compression. *Journal of Geotechnical and Geoenvironmental Engineering*, *149*(5), 04023019. https://doi.org/10.1061/JGGEFK.GTENG-10972

Anilkumar, R., Chen, Y., & Martinez, A. (2024). Plant Root-Inspired Soil Penetration in Sands Using Circumnutations for Geotechnical Site Characterization. *Geo-Congress 2024*. Geo-congress 2024, Vancouver, BC.

Anilkumar, R., & Martinez, A. (2024a). Plant root circumnutation-inspired penetration in sand and clay. *Proceedings of the 7th International Conference on Geotechnical and Geophysical Site Characterization*.

Anilkumar, R., & Martinez, A. (2024b). Experimental investigation of circumnutation-inspired penetration in sand. *Bioinspiration & Biomimetics*, *20*(1), 016006.

Bengough, A. G., Mullins, C. E., & Wilson, G. (1997). Estimating soil frictional resistance to metal probes and its relevance to the penetration of soil by roots. *European Journal of Soil Science*, *48*(4), 603–612. https://doi.org/10.1111/j.1365-2389.1997.tb00560.x

Bengough, A. G., Mackenzie, C. J., & Elangwe, H. E. (1994). Biophysics of the growth responses of pea roots to changes in penetration resistance. *Plant and Soil*, *167*, 135-141.

Boulanger, R. W., & DeJong, J. T. (2018). Inverse filtering procedure to correct cone penetration data for thin-layer and transition effects. In *Cone Penetration Testing 2018*. CRC Press.

Chen, Y., Khosravi, A., Martinez, A., & DeJong, J. (2021). Modeling the self-penetration process of a bio-inspired probe in granular soils. *Bioinspiration & Biomimetics*, *16*(4), 046012. https://doi.org/10.1088/1748-3190/abf46e

Chen, Y., & Martinez, A. (2024). DEM modelling of root circumnutation-inspired penetration in shallow granular materials. *Géotechnique*, 1–18. https://doi.org/10.1680/jgeot.22.00258

Chen, Y., Zhang, N., Fuentes, R., & Martinez, A. (2024). A numerical study on the multi-cycle self-burrowing of a dual-anchor probe in shallow coarse-grained soils of varying density. *Acta Geotechnica*, *19*(3), 1231–1250. https://doi.org/10.1007/s11440-023-02088-9

Del Dottore, E., Mondini, A., Sadeghi, A., Mattoli, V., & Mazzolai, B. (2017). An efficient soil penetration strategy for explorative robots inspired by plant root circumnutation movements. *Bioinspiration & Biomimetics*, *13*(1), 015003.

Guireli Netto, L., Barbosa, A. M., Galli, V. L., Pereira, J. P. S., Gandolfo, O. C. B., & Birelli, C. A. (2020). Application of invasive and non-invasive methods of geo-environmental investigation for determination of the contamination behavior by organic compounds. *Journal of Applied Geophysics*, *178*,104049.https://doi.org/10.1016/j.jappgeo.2020.104049

Isava, M., & Winter V, A. G. (2016). Razor clam-inspired burrowing in dry soil. *International Journal of Non-Linear Mechanics*, *81*, 30–39.

Jamiolkowski, M. (2012). Role of Geophysical Testing in Geotechnical Site Characterization. *Soils and Rocks*, *35*(2), 117–137. https://doi.org/10.28927/SR.352117

Martinez, Y. Chen, and R. Anilkumar (2024). Bio-inspired site characterization - towards soundings with lightweight equipment. 7th International Symposium on Geotechnical and Geophysical Site Characterization (ISC'7) Barcelona.

Martinez, A., Dejong, J., et al. (2022). Bio-inspired geotechnical engineering: Principles, current work, opportunities and challenges. *Géotechnique*, *72*(8), 687–705.

Moraes, M. T. de, Silva, V. R. da, Zwirtes, A. L., & Carlesso, R. (2014). Use of penetrometers in agriculture: A review. *Engenharia Agrícola*, *34*, 179–193.

Oleghe, E., Naveed, M., Baggs, E. M., & Hallett, P. D. (2017). Plant exudates improve the mechanical conditions for root penetration through soils. *Plant and Soil*, *421*, 19-30.

Purdy, C. M., Raymond, A. J., DeJong, J. T., Kendall, A., Krage, C., & Sharp, J. (2022). Life-cycle sustainability assessment of geotechnical site investigation. *Canadian Geotechnical Journal*, *59*(6), 863–877. https://doi.org/10.1139/cgj-2020-0523

Tang, Y., & Tao, J. (2022). Multiscale analysis of rotational penetration in shallow dry sand and implications for self-burrowing robot design. *Acta Geotechnica*.

Yang, X., Zhang, N., Wang, R., Martinez, A., Chen, Y., Fuentes, R., & Zhang, J.-M. (2024). A numerical investigation on the effect of rotation on the Cone Penetration Test. *Canadian Geotechnical Journal*. https://doi.org/10.1139/cgj-2023-0413.